International Journal of Nanomedicine

Dovepress
open access to scientific and medical research

Open Access Full Text Article

ORIGINAL RESEARCH

Thyroid cancer MR molecular imaging via SHP2-targeted nanoparticles

This article was published in the following Dove Press journal:
International Journal of Nanomedicine

ZhongQian Hu[1]
JiaLe Qin[2]
TianKuan Li[1]
JinHe Guo[3]

[1]Department of Ultrasound, Zhongda Hospital, Medical School, Southeast University, Nanjing, Jiangsu 210009, People's Republic of China; [2]Department of Ultrasound, Women's Hospital, School of Medicine, Zhejiang University, Hangzhou, Zhejiang 310000, People's Republic of China; [3]Center of Interventional Radiology and Vascular Surgery, Department of Radiology, Zhongda Hospital, Medical School, Southeast University, Nanjing, Jiangsu 210009, People's Republic of China

Background: Molecular imaging has generated a great demand to develop targeted contrast agents for MR imaging.

Materials and methods: In this study, we synthesized Src homology 2-containing phosphotyrosine phosphatase 2 (SHP2)-targeted and polylactic-co-glycolic acid–based nanoparticles (NPs), which encapsulated perfluoropentane and being chelated with gadolinium (Gd^{3+}) as an efficient molecular probe for targeting MR imaging on thyroid carcinoma.

Results: These NPs displayed practical properties and favorable biocompatibility in vitro. Furthermore, they showed abilities to specifically target thyroid cancer and enhance MRI as a contrast agent in both in vitro and in vivo experiments.

Conclusion: This novel MR molecular imaging based on this SHP2-targeted contrast agent provides a useful and non-invasive method for the early detection of thyroid carcinoma.

Keywords: thyroid tumor, SHP2, Gd^{3+}, nanoparticles, MR molecular imaging

Introduction

The incidence of thyroid cancer is on the rise, while there is a lack of effective means for its early detection.[1,2] Currently, the confirmed diagnosis of thyroid cancer mainly relies on fine-needle aspiration biopsy, but its application is challenged by the low sensitivity leading to a high misdiagnosis rate, as well as the risk of bleeding, infection and the recurrent laryngeal nerve damage.[3,4] Therefore, the exploration of a highly sensitive diagnostic method is urgently required. Molecular imaging technology offers a new noninvasive technique for quantitative analysis of markers at molecular or cellular levels facilitating early detection of cancer, which can overcome the shortcomings of traditional imaging methods, such as a lack of specificity and difficulties in the quantitative evaluation of tumors, and can introduce new ways of thinking and research methods in tumor research.[5–8] In recent years, MR molecular imaging with targeting probes has attracted increasing attention due to its high sensitivity and specificity.[22,23] Targeted MR molecular probes are composed of paramagnetic contrast agents and connected to ligands (such as antibodies, peptides or small-molecule compounds) with a high affinity by specific methods.[20,21]

Src homology 2-containing phosphotyrosine phosphatase 2 (SHP2) is a proven oncogene, SHP2 and other PTPs regulate many disease progress and contribute to tumorigenesis. Our previous studies have confirmed that SHP2 is overexpressed in thyroid cancer tissues and thus can be served as a sensitive marker for its detection.[9] Therefore, SHP2 antibodies can be bound to contrast agents to enable specific imaging for the purpose of early diagnosis of thyroid cancer.

Correspondence: TianKuan Li
Department of Ultrasound, Zhongda Hospital, Medical School, Southeast University, 87 Dingjiaqiao Road, Nanjing, Jiangsu 210009, People's Republic of China
Tel +86 25 8327 5402
Email ltk1105@126.com

JinHe Guo
Center of Interventional Radiology and Vascular Surgery, Department of Radiology, Zhongda Hospital, Medical School, Southeast University, 87 Dingjiaqiao Road, Nanjing, Jiangsu 210009, People's Republic of China
Tel +86 25 8327 2114
Email jinheguo@sina.com

submit your manuscript | www.dovepress.com
DovePress
http://doi.org/10.2147/IJN.S201358

MR molecular probes can be combined with paramagnetic or superparamagnetic substances to shorten the longitudinal or transverse relaxation times to enable imaging in an MR instrument.[16,17] The most commonly chelated paramagnetic substance is Gd3+.[18,19] Gd3+ has seven unpaired electrons, and its sudden release should result in being fully surrounded by water molecules and speeding up the relaxation recovery of water molecules, which show limited activity, that surround the Gd^{3+} ions, thus leading to the decline in the relaxation rate. The previous studies have confirmed that a large number of Gd^{3+}-chelating DOTA molecules can be conjugated to the surface of quantum-dot carriers to provide more Gd3+-chelating sites. Moreover, nanocarriers limit the rotation of Gd^{3+}, enhance the rigidity of the Gd^{3}+ chelates to improve the relaxation rate[26] and ensure its biosafety by effectively avoiding free Gd^{3+} ions, which may lead to serious complications such as renal fibrosis.[27]

Polylactic-co-glycolic acid (PLGA) is a biodegradable copolymer of lactic acid and glycolic acid compound with a good biological compatibility, which can be completely degraded in the body into carbon dioxide and water and has received FDA certification.[10–13] The functional groups of PLGA can be further modified, and the functional group of –COOH was the most widely used in the medical field.[14,15]

Previously, we developed SHP2-targeted perfluoropentane (PFP)/PLGA nanoparticles (NPs) as a novel molecular probe, which could be converted into microbubbles for ultrasound imaging under low-intensity ultrasound (LIFU) irradiation (1.40 w/cm^2 for 20 mins). Based on the above findings, in this study, we further fabricated SHP2-targeted PFP/PLGA NPs chelated to the paramagnetic contrast agent, Gd^{3+}, on their surface to construct a MR molecular probe (NPs-SHP2). The biocompatibility and targeting ability of this probe were preliminarily investigated in vitro. The effect of enhancing MR imaging was confirmed in an agarose gel model. After intravenous administration into mice bearing thyroid cancer, LIFU was performed to generate sonoporation effect facilitating the probe to penetrate into tumor tissue and accumulate in the local area for MR molecular imaging. Therefore, the current findings provide a novel imaging method with high sensitivity and specificity for the early detection of thyroid cancer. The schematic outline of our study is shown in Figure 1.

Materials and methods

Preparation of PLGA nanoparticles

The PFP/PLGA NPs were prepared according to the procedure as described previously.[9] In brief, 50 mg of PLGA-COOH (lactide:glycolide =50:50, MW =10,000 Da) was

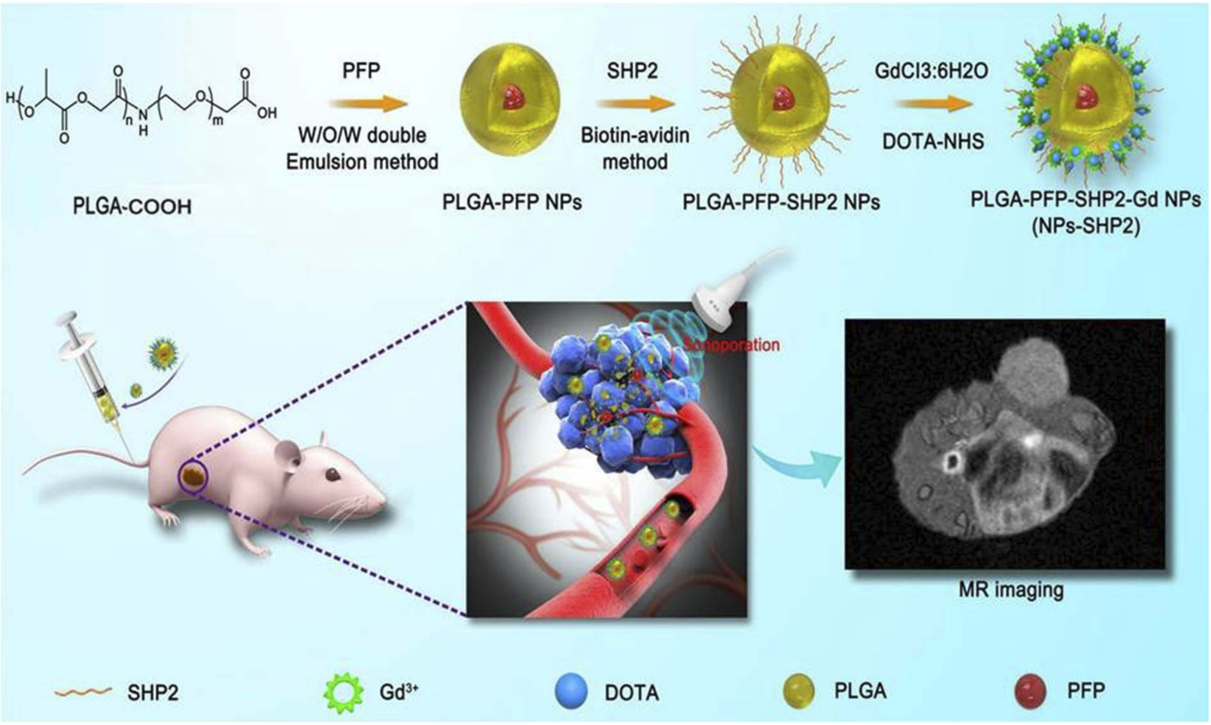

Figure 1 Schematic illustration of in vivo-induced MR imaging of a tumor employing SHP2-targeted nanoparticles.

dissolved in 1 mL of trichloromethane and mixed with 100 μL of PFP (Sigma-Aldrich Chemical Co., USA), and the primary emulsion was obtained by ultrasonic probe (VCX-130, 20 Hz, Sonics & Materials, Inc., USA) at an intensity of 100 W for 6 mins (5 s on and 5 s off). Then, 10 mL solution of 3% poly (vinyl alcohol) (MW: 25,000) was slowly added and the mixture was homogenized for 5 mins. The resulting solution was stirred for 2–4 hrs under a magnetic stirrer to make the microsphere surface coating and then the products were washed with double-distilled water three times and collected by centrifugation (5000 RPM, 5 min). To label the NPs, a small amount of DiI fluorescent dye (1 mg, DiI) was added to the $CHCl_3$ solution and covered with silver papers to prevent light exposure, and subsequently, the same procedures were adopted as that detailed above.

Preparation and characterization of MR molecular probe

Preparation of NPs-SHP2

To functionalize the NPs, the above-prepared PFP/PLGA NPs were dispersed in 5 mL PBS (pH=6.0), and appropriate amounts of the coupling activators EDC (0.1 mL, 50 mg/mL) and NHS (0.1 mL, 50 mg/mL) were dissolved in 1 mL of double-distilled water. After being reacted at room temperature for 2 hrs, the resulting NPs were collected by centrifugation, washed with double-distilled water and dispersed in PBS (pH=8.0). Then, 200 μL solution with SHP2 antibody was added and reacted at room temperature for 2 hrs, and the SHP2-targeted PFP/PLGA NPs (NPs-SHP2) were eventually obtained and dispersed in PBS again.

Preparation of NPs-SHP2. $Gd3^+$

A total of 500 μL polyethyleneimine was diluted in 2 mL of double-distilled water and added to the above NPs-SHP2 emulsion. The pH was adjusted to 8.0 by dilute hydrochloric acid. The mixture was shaken evenly and allowed to react at room temperature for 2 h. DOTA-NHS (30 nmol) was added and completely reacted over 2 hrs, and then the resulting NPs were dispersed in PBS solution after washing (pH=8.0). $GdCl_3.6H_2O$ (30 nmol) was dissolved in 1 mL of double-distilled water and slowly added to the above solution so that DOTA could fully chelate with Gd^{3+}. After centrifugation and purification, SHP2-targeted PFP/PLGA NPs that chelated with Gd^{3+} (NPs-SHP2. Gd^{3+}) were obtained as a novel MR molecular probe, and the final product was dispersed in 5 mL of PBS. The particle distribution and morphological characteristics were observed under optical microscopy (CKX41, Olympus, Tokyo, Japan). The mean particle size and zeta potential of NPs-SHP2. Gd^{3+} were determined by dynamic light scattering (DLS) (Malvern Instruments, Pennsylvania, PA, USA).

Cell culture

Nthori3-1 and SW579 cell lines were cultured in RPMI-1640, with 10% FBS at 37°C and 5% CO_2, purchased from the Institute of Biochemistry and Cell Biology, Chinese Academy of Sciences (Shanghai, China). The use of the cell lines was approved by Southeast University Institutional Review Board or Ethics Committee and was authenticated by STR profile (SW579, Cat.No:CC-Y1501, Nthori3-1, Cat. No: C1002).

Animal model

Animal ethical and legal protocols were approved prior to the commencement of this study by the Animal Studies Core Facility at the Southeast University. All experiments were performed following the Southeast University and national guidelines and regulations.

SW579 cells were collected, centrifuged and resuspended in PBS in 1.5-mL tubes (3×10^6 cells per tube) and then inoculated into the right dorsal flank of mice to build a mouse model of thyroid cancer following the experimental protocol as described in previous reports.[9] The mice were performed MR imaging 3 weeks after tumor inoculation.

Cytotoxicity test in Nthori3-1 cells from normal thyroid tissue

MTS method was employed to evaluate the effects of NPs-SHP2. Gd^{3+} on cell proliferation. Nthori3-1 cells from normal thyroid tissue were plated at a density of 5×10^3 cells/well in 96-well plates. Twenty-four hours later, different concentrations of NPs-SHP2. $Gd3^+$ (5 pmol/mL, 10 pmol/mL, 15 pmol/mL and 20 pmol/mL) were added and divided into four groups. A negative control of RPMI-1640 medium and positive control of 0.5 μmol/mL doxorubicin were also placed simultaneously. The cells were allowed to grow for 48 hrs, and then 10 μL/well MTS was added and the cells were cultured for 3 hrs at the regular condition. The absorbance of each well was measured by spectrophotometer. The data are expressed as the OD values at 490 nm among all the groups and compared. The experiment was repeated in triplicate.

Effect on apoptosis in thyroid cancer cells

SW579 cells were collected 72 hrs after treatment with RPMI-1640, non-targeted NPs (20 pmol/mL), targeted NPs (20 pmol/mL) and doxorubicin (0.5 μmol/mL). The procedure for immunoblotting has been previously described.[9] In brief, aliquots of protein samples (15 μg) were separated on an SDS-polyacrylamide gel by electrophoresis. The separated proteins were transferred to nitrocellulose membranes. The membranes were blocked with either 5% nonfat milk in 0.01 M PBS (pH 7.4) or 0.05% Tween-20 (TPBS) at room temperature for 1 hr. Subsequently, the membranes were probed with three types of primary antibodies (BAX, Caspas-3, Bcl-2) directed against the target proteins overnight at 4°C. After three quick washes in TPBS, the membranes were incubated with a secondary antibody conjugated to horseradish peroxidase (Amersham, Arlington Hts, IL). The immune complexes were detected by the enhanced chemiluminescence method (Amersham).

In vitro targeting ability

SW579 cells were seeded into six-well plates for 24 h or until 50% confluence was reached. The cells were treated with either NPs-SHP2. $Gd3^+$ or non-targeting control NPs (NPs-Control) at 37°C for 30 mins, and then DiO (Keygen, China) was added to was stained the cell membrane. The NPs in these two groups were stained with Dil (Keygen, China) in advance. Finally, the cells were washed, fixed and then imaged under confocal fluorescent microscope.

In vitro MR imaging

Different concentrations (3.0, 2.0, 1.0, 0.50 and 0.25 mmol/L, 1% agarose gel) of NPs-SHP2. $Gd3^+$ were added to an agarose gel model, and small-animal MR imager was used for scanning, image collection and analysis.

MR molecular imaging

Three weeks after tumor inoculation, the mice were injected with 0.1 mL of either NPs-SHP2 or NPs-Control through the caudal vein and divided into two groups at random. Then, the tumor site in mice was irradiated with LIFU 5 mins after injection, and MR scanning was performed immediately. The signal intensity in the tumor area was observed and analyzed.

Statistical analysis

All data are expressed as the means ± SD. Means were compared using one-way ANOVA and Student's *t*-test, and *P*-values <0.05 were considered statistically significant.

Results

Preparation and characterization of NPs-SHP2. $Gd3^+$

NPs-SHP2 appeared as a white emulsion and would be layered after 10–15 mins of standing. Under optical and fluorescent microscope, the NPs showed a spherical shape with regular morphology, well-distributed sizes and good dispersity (Figure 2A). The diameter of the NPs was centered around a single peak with a mean diameter of 535.72 nm (±40.7 nm) (Figure 2B), and they had an electric potential of 14.23±8.69 mV (Figure 2C).

Cytotoxicity of NPs-SHP2. $Gd3^+$ in Nthori3-1 cells

We also tested the cell proliferation of NPs in cells by MTS and fluorescence microscopy imaging techniques. For MTS, Nthori3-1 cells were treated with NPs-SHP2. $Gd3^+$ at different concentrations. The MTS method was employed to observe the effect of SHP2-targeting NPs on the proliferation of normal thyroid cell lines. As shown in Figure 3A, the growth and proliferation of doxorubicin-treated cells in the positive control group were significantly inhibited, and the trends of cell growth and proliferation did not change significantly among other groups (*P<0.05). This indicated that the targeting NPs had no obvious effects on cell growth and had good biocompatibility.

Apoptosis of SW579 cells after treatment

The expression of the apoptotic protein in SW579 thyroid cells was assessed after treatment with 20 pmol/mL of the targeting NPs, 20 pmol/mL NPs, 0.5 μmol/mL doxorubicin and RPMI-1640 individually to further examine the pathways associated with the cytotoxic and antiproliferative effects (Figure 3B and C). The cells were incubated with NPs for 72 hrs, and immunoblot analysis was performed using antibodies against apoptotic protein B-cell lymphoma 2 (Bcl2), caspase-3 and Bcl2-associated X protein (BAX) (Figure 3B and C). The results showed a significant increase in BAX and caspase-3 protein expression in cells treated with doxorubicin compared to the expression in the control group and targeting NP-treated cells (**P<0.01). In contrast, a decrease in Bcl2 protein expression was observed in cells treated with doxorubicin while no reduction was observed in the other groups. These results showed that the targeted NPs alone had no effect on cell growth and apoptosis.

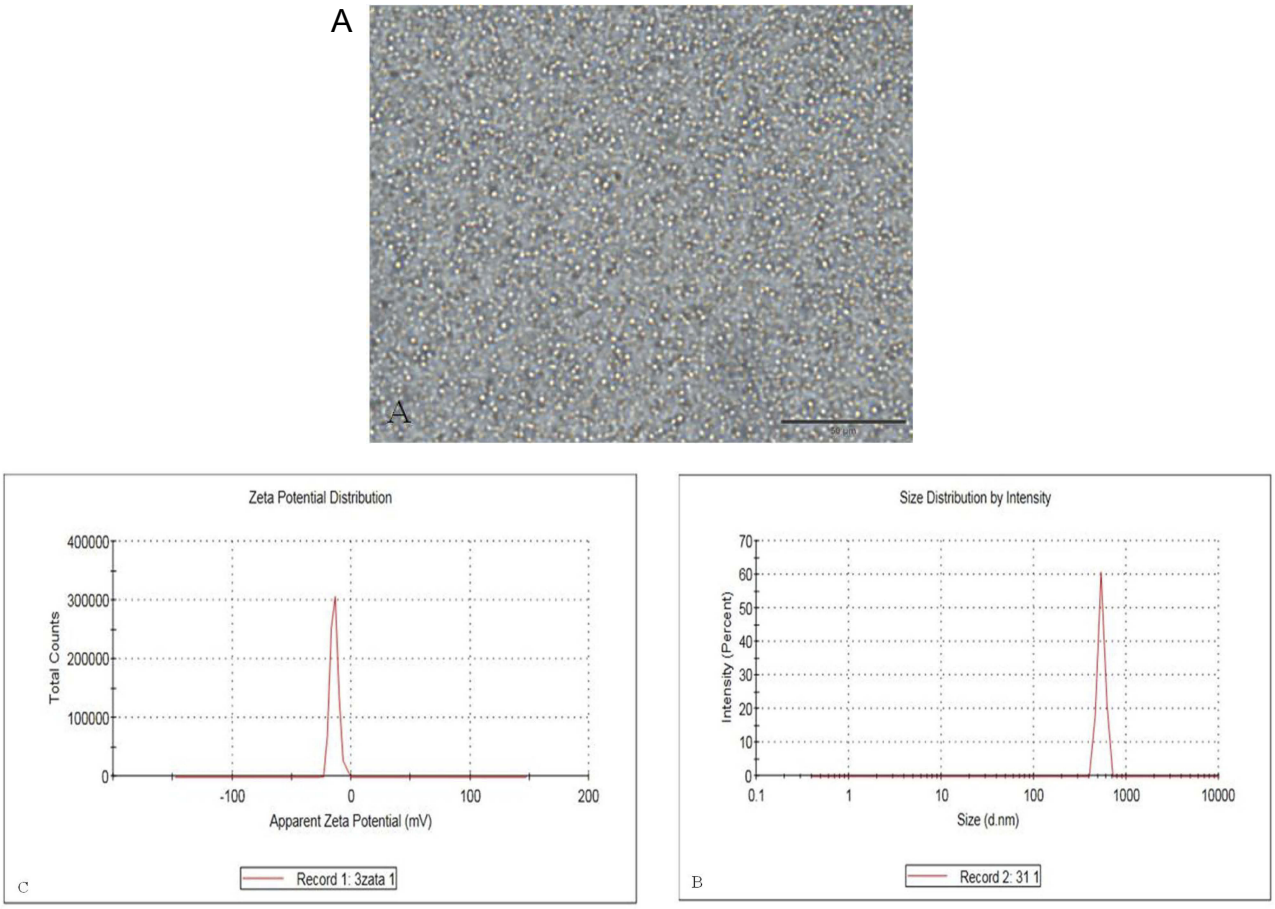

Figure 2 Characterization of the SHP2-targeted nanoparticles. (**A**) Brightfield optical microscopy image, (**B**) size distribution and (**C**) zeta potential.

In vitro MR imaging

Targeting NPs at different concentrations were scanned under MR, and it was found that the T1 signal intensity increased significantly with increasing NP concentration (Figure 4). In this case, the amount of T1 signal intensity increase turned out to be positively correlated with the increase in the Gd^{3+} concentration, indicating that the T1 signal had a concentration dependence within a certain range (*P<0.05).

In vitro targeting ability

SW579 cells were treated previously with targeted and nontargeted NPs, respectively. From the fluorescence imaging results, SW579 cells showed evident green fluorescence in the cell membrane as stained by DiO. Moreover, a large amount of red signal was found around cells after treated with NPs-SHP2. Gd^{3+} (Figure 5A). In contrast, the cells treated with nontargeting NPs exhibited little red fluorescence around the cell membrane (Figure 5B, **P<0.01). These results indicate that NPs-SHP2. Gd^{3+} had targeting ability to thyroid cancer cells.

MR molecular imaging in vivo

Targeting and nontargeting NPs were injected into nude mice through the tail vein. To promote NP uptake into the tumor tissue, the tumors were irradiated with LIFU 5 mins after injection to induce sonoporation. MR-enhanced imaging results showed (Figure 6A and B) that the targeting NP group exhibits a remarkable capability to enhance MR imaging in vivo and has a relatively longer in vivo retention time compared to that of the nontargeting NP tumor signal intensity (*P<0.05).

Discussion

PLGA is safe, nontoxic, biocompatible and stable polymer material which can be degraded into CO_2 and H_2O in vivo.[10–12] PLGA NPs have been developed and chemically modified by ligands or antibodies as molecular probes for targeted imaging. From previous reports, SHP2 antibody

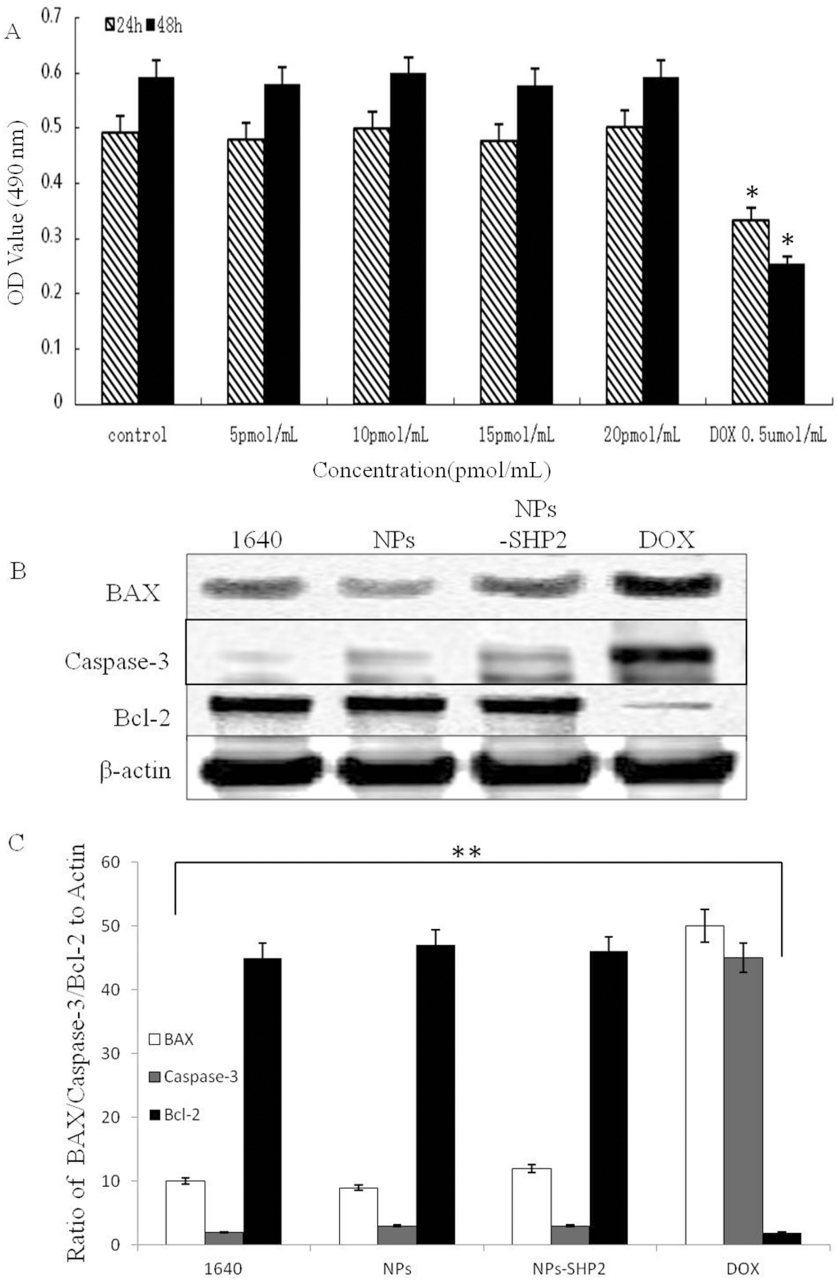

Figure 3 In vitro cytotoxicity experiments. (**A**) The proliferative effects of SHP2-targeted nanoparticles on Nthori3-1 cells. (**B** and **C**) After treatment with NPs in SW579 cells, SHP2-NPs and DOX, BAX and caspase-3 expression were significantly increased, while bcl-2 expression was decreased compared with any other group (**P<0.01, *P<0.05).

was successfully conjugated onto the surface of PLGA NPs to target SHP2-expressed tumor cells.[9] Moreover, PLGA NPs wrapping paclitaxel were also functionalized with folate and applied to targeted tumor therapy.[24,25] We previously developed phase-changeable, SHP2-targeted PLGA NPs encapsulating PFP to enhance ultrasound imaging in mouse thyroid cancer model. In this study, the above SHP2-targeted PLGA NPs were further chelated with Gd^{3+} to fabricate a novel molecular probe NPs-SHP2.Gd^{3+} for targeted MR imaging. In addition, this new probe did not show an obvious effect on cell growth or apoptosis in vitro, exhibiting favorable biocompatibility for further application as side effects from free Gd^{3+} ions were avoided.

Gd-DOTA, with its T1 enhancement effects and stable dynamics, is often selected as an excellent contrast agent for MR molecular imaging.[28] In vitro experiment, the molecular probe NPs-SHP2.$Gd3^{+}$ presented a slightly higher signal under MR even at a pretty low

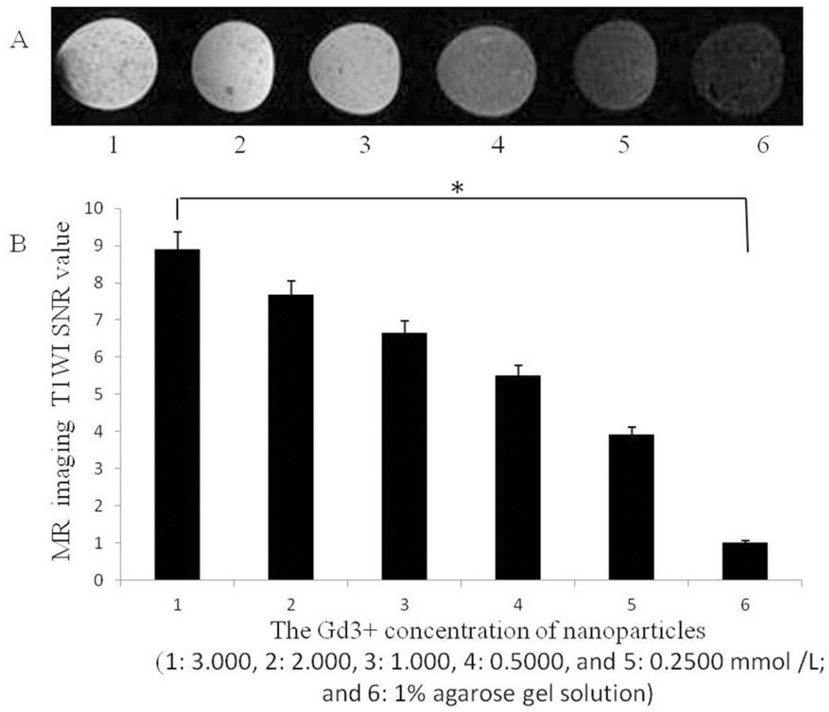

Figure 4 (**A**) T1-weighted images of nanoparticles with different Gd3+ concentrations and (**B**) the corresponding SNR (the Gd3+ concentration of nanoparticles was 1: 3.000, 2: 2.000, 3: 1.000, 4: 0.5000 and 5: 0.2500 mmol /L; and 6: 1% agarose gel solution (*P<0.05).

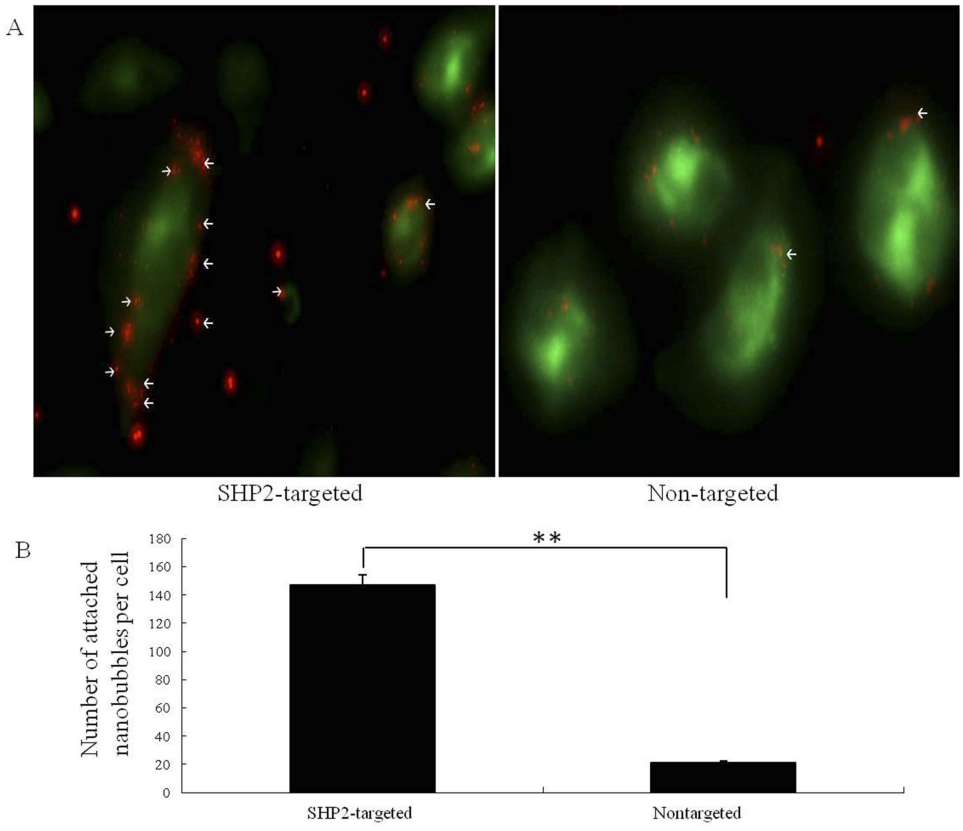

Figure 5 In vitro targeting ability experiments. (**A**) Fluorescence images showing the results of binding with SW579 cells for SHP2-targeted and nontargeted nanoparticles. (**B**) After SHP2-targeted nanoparticle treatment, the red fluorescence signal around the cells increased significantly compared with that obtained after treatment the nontargeted nanoparticles (control) (**P<0.01).

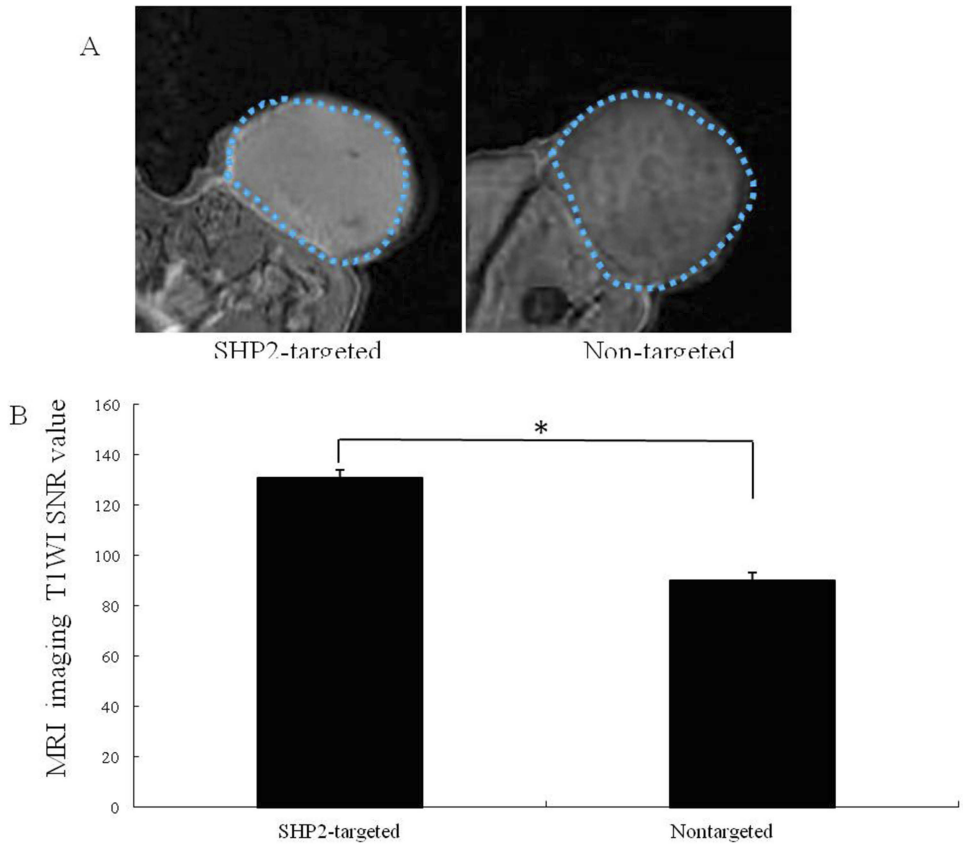

Figure 6 (**A**) Subcutaneous human thyroid carcinoma xenograft tumor (blue dashed line) imaged with contrast-enhanced MR after the injection of SHP2-targeted and nontargeted nanoparticles and LIFU irradiation for 5 mins. (**B**) The imaging signal obtained after SHP2-targeted nanoparticle injection was substantially higher than that obtained after nontargeted nanoparticle (control) injection (*P<0.05).

Gd^{3+} concentrations of 0.5000 mmol/L and produced good MR imaging. Moreover, the signal to noise ratio of the MR imaging from NPs-SHP2.$Gd3^{+}$ was enhanced with the increase of Gd^{3+} concentration, indicating a concentration-dependent effect within the range from 3.0 to 0.25 mmol/L.

As observed by laser confocal microscopy, NPs-SHP2.$Gd3^{+}$ distinctly targeted SW579 cells while nontargeted NPs did not show this phenomenon, which was consistent with the previous findings as we reported,[9] indicating that the addition of paramagnetic Gd^{3+} contrast agent did not affect the targeting ability of this molecular probe. In vivo experiment, under LIFU irradiation, NPs-SHP2.$Gd3^{+}$ were facilitated to pass through tumor vascular endothelial gap, penetrate into tumor tissue and accumulate in tumor area due to enhanced permeability and retention effect, then they actively targeted thyroid cancer cells allowing for MR molecular imaging.

In short, we successfully developed PLGA NPs functionalized with SHP2 and paramagnetic Gd^{3+} contrast agent as a novel MR molecular probe in this study. This probe showed good biocompatibility, highly targeting ability to thyroid cancer cells and contrast-enhanced effect on MR imaging and was worthy of further study in future. The preliminary findings lay a foundation to explore a noninvasive imaging method for the early diagnosis of thyroid cancer based on the high expression of SHP2.

Acknowledgment

This work was supported by grants from the National Natural Sciences Foundation of China (81971628 and 81501444).

Author contributions

All authors contributed to data analysis, drafting and revising the article, gave final approval of the version to be published, and agree to be accountable for all aspects of the work.

Disclosure

The authors report no conflicts of interest in this work.

References

1. Yoo J, Ahn HS, Kim SJ, Park SH, Seo M, Chong S. Evaluation of diagnostic performance of screening thyroid ultrasonography and imaging findings of screening-detected thyroid cancer. *Cancer Res Treat*. 2018;50(1):11–18. doi:10.4143/crt.2016.600
2. Lan XB, Zhang H. An introduction of surgical update in 2015 American Thyroid Association Management Guidelines for Adult Patients with Thyroid Nodules and Differentiated Thyroid Cancer. *Zhonghua Wai Ke Za Zhi*. 2016;54(3):172–176. doi:10.3760/cma.j.issn.0529-5815.2016.03.004
3. Stefano V, Giuliano S, Francesco R, et al. Cancer rate of the indeterminate lesions at low or high risk according to italian system for reporting of thyroid FNA. *Front Endocrinol (Lausanne)*. 2018;9:371. doi:10.3389/fendo.2018.00420
4. Nikiforova MN, Mercurio S, Wald AI, et al. Analytical performance of the ThyroSeq v3 genomic classifier for cancer diagnosis in thyroid nodules. *Cancer*. 2018;124:1682–1690. doi:10.1002/cncr.v124.8
5. Di HT, Wahl RL. Molecular imaging in thyroid cancer. *Cancer Imaging Off Publ Int Cancer Imaging Soc*. 2010;10(1):1.
6. Ahn BC. Personalized medicine based on theranostic radioiodine molecular imaging for differentiated thyroid cancer. *Biomed Res Int*. 2016;2016(5):1–9.
7. Wong KK, Dvorak RA, Marzola MC, Grassetto G, Gross MD, Rubello D. Molecular imaging in the management of thyroid cancer. *Q J Nucl Med Mol Imaging*. 2011;55(5):541–559.
8. Santhanam P, Solnes LB, Rowe SB. Molecular imaging of advanced thyroid cancer: iodinated radiotracers and beyond. *Medical Oncology*. 2017;34(12):189. doi:10.1007/s12032-017-1051-x
9. Zhongqian H, Yang B, Tiankuan L, Jia L. Thyroid cancer detection by ultrasound molecularimaging with SHP2-targeted perfluorocarbon nanoparticles. *Contrast Media Mol Imaging*. 2018;7.
10. Sun Y, Zheng Y, Ran H, et al. Corrigendum to "Superparamagnetic PLGA-iron oxide microcapsules for dual-modality US/MR imaging and high intensity focused US breast cancer ablation" [Biomaterials 33 (2012) 5854-5864]. *Biomaterials*. 2015;64:1. doi:10.1016/j.biomaterials.2015.06.021
11. Devulapally R, Foygel K, Sekar TV, Willmann JK, Paulmurugan R. Gemcitabine and antisense-microRNA co-encapsulated PLGA-PEG polymer nanoparticles for hepatocellular carcinoma therapy. *ACS Appl Mater Interfaces*. 2016;8(49):33412. doi:10.1021/acsami.6b08153
12. Devulapally R, Lee T, Barghava-Shah A, et al. Ultrasound-guided delivery of thymidine kinase-nitroreductase dual therapeutic genes by PEGylated-PLGA/PIE nanoparticles for enhanced triple negative breast cancer therapy. *Nanomedicine*. 2018;13(9):1051–1066. doi:10.2217/nnm-2017-0328
13. Devulapally R, Sekar NM, Sekar TV, et al. Polymer nanoparticles mediated co-delivery of antimir-10b and antimiR-21 for achieving triple negative breast cancer therapy. *ACS Nano*. 2015;9(3):2290–2302. doi:10.1021/nn507465d
14. Noormehr H, Zavaran HA, Soudi S, Beyzay F. Enhancement of Th1 immune response against Leishmania cysteine peptidase A, B by PLGA nanoparticle. *Int Immunopharmacol*. 2018;59:97–105. doi:10.1016/j.intimp.2018.03.012
15. Wang T, Hurwitz O, Shimada SG, et al. Anti-nociceptive effects of bupivacaine-encapsulated PLGA nanoparticles applied to the compressed dorsal root ganglion in mice. *Neurosci Lett*. 2018;668:154–158. doi:10.1016/j.neulet.2018.01.031
16. Burks SR, Barth ED, Martin SS, et al. Targeted delivery of molecular probes for in vivo, electron paramagnetic resonance imaging. 26th Southern Biomedical Engineering Conference SBEC 2010, April 30 - May 2, 2010, College Park, Maryland, USA; 2010.
17. Mulder WJM, Koole R, Brandwijk RJ, et al. Quantum dots with a paramagnetic coating as a bimodal molecular imaging probe. *Nano Lett*. 2006;6(1):1–6. doi:10.1021/nl051935m
18. Li Q, Li C, Tong W. Nile red loaded PLGA nanoparticles surface modified with Gd-DTPA for potential dual-modal imaging. *J Nanosci Nanotechnol*. 2016;16(6):5569–5576. doi:10.1166/jnn.2016.11735
19. Amanlou M, Siadat SD, Ebrahimi SE, et al. Gd3+-DTPA-DG: novel nanosized dual anticancer and molecular imaging agent. *Int J Nanomedicine*. 2011;6(1):747–763. doi:10.2147/IJN.S17648
20. Wu B, S T L, Deng K, et al. MRI-guided targeting delivery of doxorubicin with reduction-responsive lipid-polymer hybrid nanoparticles. *Int J Nanomedicine*. 2017;12:6871–6882. doi:10.2147/IJN.S143048
21. Jing Z, Hao G, Yao C, et al. Paramagnetic albumin decorated CuInS2/ZnS QDs for CD133+ glioma bimodal MR/fluorescence targeted imaging. *J Mater Chem B*. 2016;4(23):4110–4118. doi:10.1039/C6TB00834H
22. Park KE, Noh YW, Kim A, Lim YT. Hyaluronic acid-coated nanoparticles for targeted photodynamic therapy of cancer guided by near-infrared and MR imaging. *Carbohydr Polym*. 2017;157:476–483. doi:10.1016/j.carbpol.2016.10.015
23. Alberti D, Protti N, Franck M, et al. Theranostic nanoparticles loaded with imaging probes and rubrocurcumin for combined cancer therapy by folate receptor targeting. *Chemmedchem*. 2017;12(7):502. doi:10.1002/cmdc.201700368
24. Jianxin L, Fenfen X, ZhongQian H, et al. Low intensity focused ultrasound-activatable nanodroplets as a theranostic agent for non-invasive cancer molecular imaging imaging and drug delivery. *Biomater Sci*. 2018;6:2838–2849. doi:10.1039/c8bm00726h
25. Turino LN, Ruggiero M, Stefania R, et al. Ferritin decorated PLGA/Paclitaxel loaded nanoparticles endowed with an enhanced toxicity towards MCF-7 breast tumour cells. *Bioconjug Chem*. 2017;28(4):1283–1290. doi:10.1021/acs.bioconjchem.7b00096
26. Ratzinger G, Agrawal P, Körner W, et al. Surface modification of PLGA nanospheres with Gd-DTPA and Gd-DOTA for high-relaxivity MRI contrast agents. *Biomaterials*. 2010;31(33):8716–8723. doi:10.1016/j.biomaterials.2010.07.095
27. Chen Z, Yu D, Liu C, et al. Gadolinium-conjugated PLA-PEG nanoparticles as liver targeted molecular MRI contrast agent. *J Drug Target*. 2011;19(8):657–665. doi:10.3109/1061186X.2010.531727
28. Gill MR, Menon JU, Jarman PJ, et al. 111In-labelled polymeric nanoparticles incorporating a ruthenium-based radiosensitizer for EGFR-targeted combination therapy in oesophageal cancer cells. *Nanoscale*. 2018;10:10596–10608. doi:10.1039/C7NR09606B